Axial Momentum Theory for Turbines with Co-axial Counter Rotating Rotors

Chantharasenawong C.*, Suwantragul B. and Ruangwiset A.

Department of Mechanical Engineering, King Mongkut's University of Technology Thonburi, Bangkok, Thailand
*Corresponding author: chawin.cha@kmutt.ac.th

Abstract: This research aims to optimise the design of a co-axial twin counter rotating rotor horizontal axis turbine. The rotors are modeled as actuator discs positioned inside two concentric stream tubes. The flow in the inner stream tube passes through the inner region of the upstream rotor and the stream tube cross section area expands to cover the entire downstream rotor. The flow in the outer stream tube passes through the external part up to the blade tip of the upstream rotor. Using the axial momentum equation in conjunction with the mass conservation equation reveals that the turbine maximum power coefficient is 81.4%. This is achieved when the inner part of the upstream rotor has zero solidity and covers 58% of the total swept area or corresponding to 76.2% of the diameter of the downstream rotor. In practice, this part of the turbine blade is designed to generate minimum drag as its function is only to support the blade tip and not to extract the fluid energy itself. The turbine blades in the outer region of the upstream rotor are designed using Betz theory which specifies the local axial flow velocity to be 2/3 of the free stream. The local axial flow velocity at the downstream rotor is 0.582 of the free stream velocity.

Keywords: Horizontal axis turbine, co-axial counter rotating rotors

1. INTRODUCTION

Since its introduction in 1933, the Betz theory [1] for turbine has been fundamental in turbine development history. The theory itself comprises of an analysis of axial momentum equation together with the mass continuity equation. The power developed in the turbine shaft when compared to the fluid power is usually presented in the form of power coefficient, such as

$$C_P = \frac{P}{0.5\rho A V^3} \qquad (1)$$

where

C_P	denotes power coefficient of the turbine
P	denotes the developed power (watts)
ρ	denotes the fluid density (kg/m^3)
A	denotes the turbine swept area (m^2)
V	is the flow speed past the rotor (m/s)

The power coefficient is a function of the instantaneous flow speed past the rotor. The flow speed of $\frac{2}{3}V_\infty$, in another words the flow speed behind the rotor is $v = \frac{1}{3}V_\infty$, corresponds to the maximum power coefficient which can be generated. This is also known as the Betz limit. The value of the maximum power coefficient is $C_{P\max} = \frac{16}{27}$ or 59.3%. This theory is often used in conjunction with the blade element theory in rotor blade design applications.

Newman [2] proposed a method to analyse the power coefficient of a horizontal axis turbine which consists of two rotor discs in series. It was found that the maximum power coefficient would increase to $C_{P\max} = \frac{16}{25}$ or 64% of the fluid power. The conditions at which maximum power is generated require the flow speed past the first rotor to be $0.8V_\infty$ and the flow speed past the second (downstream) rotor to be $0.4V_\infty$. Subsequently, Newman [3] extended the theory to accommodate for calculation of power coefficient of horizontal axis turbine with infinite number of rotor discs in series and found that the maximum power coefficient would increase to $C_{P\max} = \frac{2}{3}$ or 66.67% of the fluid power.

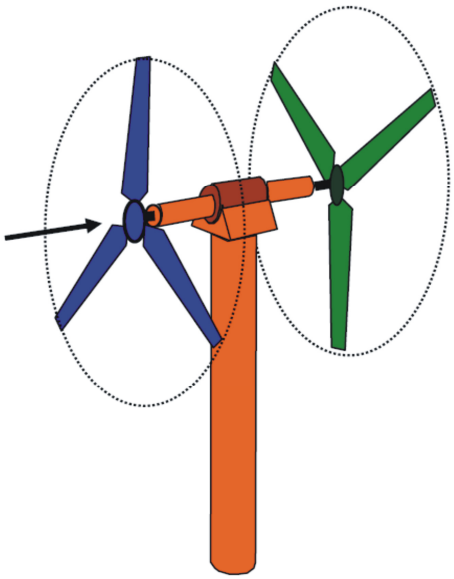

Fig.1 Illustration of a co-axial twin rotor horizontal axis turbine

Apart from theoretical advances in turbine power generation computation, there are also significant developments in designs, such as horizontal axis turbine with multiple counter rotating rotor discs. Figure 1 shows an illustration of a horizontal axis turbine with two rotor discs. The first (upstream) rotor converts part of the fluid energy into kinetic energy. The flow speed aft of the first rotor would drop compared to the free stream velocity but there is still enough energy in the flow to be harnessed by the second rotor disc which is situated downstream of the first rotor disc. The kinetic energy from the shafts of both rotors would finally be converted into electrical energy. It is common to employ the

kinetic energy from the first rotor disc to drive the rotor of the generator, while the kinetic energy from second rotor disc is used to drive the stator of the generator.

Ushiyama et al. [4] developed and built a counter rotating turbine model. They tested their model with 3, 4 and 6 blades on the 0.6m diameter upstream rotor, and with 2 and 3 blades at the 1.2m diameter downstream rotor. They recorded an increase in turbine power coefficient and relative RPM compared to conventional single rotor turbines, and hence recommended further work in their design.

Jung et al. [5] designed a co-axial counter rotating rotor horizontal axis wind turbine, which was rated at 30kW at airspeed of 10.6m/s. The main (downstream) rotor had a diameter of 11m and the auxiliary (upstream) rotor had a diameter of 5.5m. The main rotor rotated with half the speed of the auxiliary rotor. The mechanical power output of both rotors was combined by a series of gears and was finally used to drive a generator. They found that a turbine with two rotors produced higher power than a single rotor turbine, depending on the distance between the rotors. It was found that there is a 21% increase in power coefficient (up to $C_P = 0.50$) when the distance between the rotors is half of the main rotor.

Kanemoto and Galal [6] proposed a twin rotor in series turbine for use with synchronous generators. The power developed by the upstream rotor would drive the internal armature while the downstream rotor would provide power for the external armature. The upstream rotor of their turbine model had a 550mm diameter and the downstream rotor had a 390mm diameter. At low flow speed, both rotors initially rotated in the same direction and the downstream rotor would rotate at a higher speed due to its smaller size. As the flow speed increased, the rotational speed of the downstream rotor would decrease. The authors also suggested that the optimum number of turbine blades is three for the upstream rotor and between four to six blades for the downstream rotor. The main advantages of this type of wind turbine are higher power generation than traditional single rotor systems and the constant output in the rated operation mode without the installation of brakes or pitch control mechanism.

Shen et al. [7] numerically analysed the efficiency of a turbine with two counter rotating rotors. They used the characteristic curves of the three-bladed Nordtank 500kW turbine in their work. It was found that yearly electrical power generation of the turbine with two counter rotating rotors would be 43% higher than a conventional turbine.

Clarke et al. [8] developed a counter rotating marine current turbine specifically for uses in straights with high velocity current flows. They discovered that the counter rotating turbine generated higher power and almost zero reaction torque on the supporting structures. Another desirable feature is that there is near zero swirl in the wake.

Theoretical analysis suggests that a turbine with two counter rotating rotors will increase the maximum power coefficient by 8% compared to a single rotor turbine. However, many experimental results have shown that the increase can be as high as 21%. Hence this research main interest is to determine the optimum design of a turbine with two counter rotating rotors and the optimum wind speed using a mathematical model based on the axial momentum theory.

2. METHODOLOGY

The actuator disc theory [1] will be used to analyse the power coefficient of the horizontal axis turbine with two rotors in series.

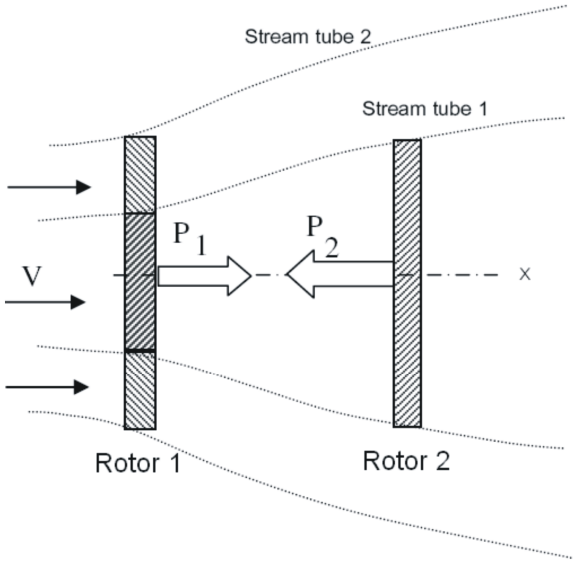

Fig.2 Diagram of a turbine with two co-axial rotors

The diagram in figure 2 shows a side view cross section of a horizontal axis turbine with two rotors in series exposed to a horizontal air flow of speed *V*. The upstream and downstream rotors will be called rotor 1 and rotor 2, respectively. Rotor 1 extracts the wind energy from the flow of speed *V* and converts it to kinetic energy P_1. It has a cross section area A_1 which consists of two regions namely the inner circular part of area A_1 and the outer ring-shaped part of area A_2. The two regions of the swept area are separated by stream tube 1 (See figure 2). The cross section area of this stream tube increases downstream to cover the entire swept area of rotor 2, A_2. The power generated by the inner and outer regions of rotor 1 and by rotor 2 are denoted $P_{1-Inner}$, $P_{1-Outer}$, and P_2, respectively.

The flow of speed *V* passes through the inner region of rotor 1 with a local speed of $(1-a)V$ which causes a pressure drop $\Delta p_{1-Inner}$ across the rotor within stream tube 1. This also causes a change in flow speed, hence in the region downstream of rotor 1 the flow speed is represented by $(1-b)V$. The pressure at this part of the stream tube is equal to the atmospheric pressure. (See figure 3b for axial pressure profile) Flow speed drops further when it passes through (the entire area of) rotor 2 where the local speed is $(1-b-c)V$. The pressure drop across rotor 2 is given by Δp_2 and the final flow speed downstream of rotor 2 is given

by $(1-b-d)V$. The pressure at this position must be equal to the atmospheric pressure.

The ring shaped outer region of the swept area of rotor 1, bound by stream tubes 1 and 2, has a local flow speed of $(1-e)V$. This results in a pressure drop $\Delta p_{1-Outer}$ across the rotor. The flow in this stream tube will decelerate further downstream until the speed is $(1-f)V$ where the pressure is equal to the atmospheric pressure.

See figure 3a for the numbering system of regions used in the following section.

The axial load generated at the inner region of rotor 1 is given by

$$T_{1-Inner} = A_{1-Inner}.\left(p^{+}_{1-Inner} - p^{-}_{1-Inner}\right) \quad (2)$$

The axial load generated at the outer region of rotor 1 is given by

$$T_{1-Outer} = A_{1-Outer}.\left(p^{+}_{1-Outerr} - p^{-}_{1-Outer}\right) \quad (3)$$

The axial load generated at rotor 2 is given by

$$T_2 = A_2.\left(p_2^{+} - p_2^{-}\right) \quad (4)$$

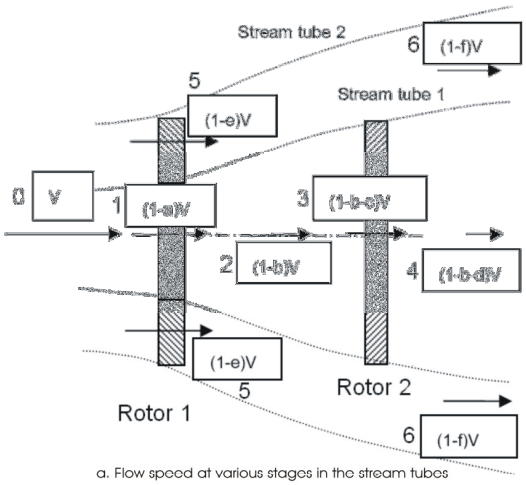

a. Flow speed at various stages in the stream tubes

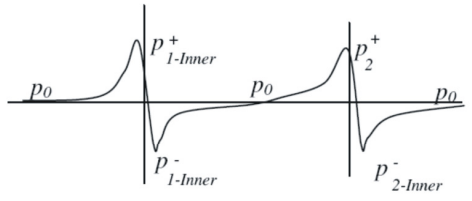

b. Pressure profile in stream tube 1

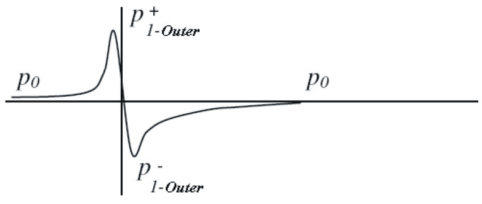

c. Pressure profile in stream tube 2

Fig.3 Flow velocities and pressure at various stages

Applying the Bernoulli's equation at region 0 and a position immediately upstream of region 1 to obtain

$$p_0 + 0.5\rho V^2 = p^{+}_{1-Inner} + 0.5\rho(1-a)^2V^2 \quad (5)$$

Applying the Bernoulli's equation at a position immediately downstream of region 1 and region 2 to obtain

$$p^{-}_{1-Inner} + 0.5\rho(1-a)^2V^2 = p_0 + 0.5\rho(1-b)^2V^2 \quad (6)$$

Applying the Bernoulli's equation at region 2 and a position immediately upstream of region 3 to obtain

$$p_0 + 0.5\rho(1-b)^2V^2 = p_2^{+} + 0.5\rho(1-b-c)^2V^2 \quad (7)$$

Applying the Bernoulli's equation at a position immediately downstream of region 3 and region 4 to obtain

$$p_2^{-} + 0.5\rho(1-b-c)^2V^2 = p_0 + 0.5\rho(1-b-d)^2V^2 \quad (8)$$

Applying the Bernoulli's equation at region 0 and immediately upstream of region 5 to obtain

$$p_0 + 0.5\rho V^2 = p^{+}_{1-Outer} + 0.5\rho(1-e)V^2 \quad (9)$$

Applying the Bernoulli's equation at a position immediately downstream of region 5 and region 6 to obtain

$$p^{-}_{1-Outer} + 0.5\rho(1-e)^2V^2 = p_0 + 0.5\rho(1-f)^2V^2 \quad (10)$$

Combining equations 5 and 6 to obtain

$$p^{+}_{1-Inner} - p^{-}_{1-Inner} = 0.5\rho\left[1-(1-b)^2\right]V^2$$

Combining equations 7 and 8 to obtain

$$p_2^{+} - p_2^{-} = 0.5\rho\left[(1-b)^2 - (1-b-d)^2\right]V^2$$

Combining equations 9 and 10 to obtain

$$p^{+}_{1-Outer} - p^{-}_{1-Outer} = 0.5\rho\left[1-(1-f)^2\right]V^2$$

The expressions for axial loads (equations 2–4) can be rewritten as

$$T_{1-Inner} = 0.5\rho A_{1-Inner}\left[1-(1-b)^2\right]V^2 \quad (11)$$

$$T_2 = 0.5\rho A_2\left[(1-b)^2 - (1-b-d)^2\right]V^2 = 0.5\rho A_2\left[2d - 2bd - d^2\right]V^2 \quad (12)$$

$$T_{1-Outer} = 0.5\rho A_{1-Outer}\left[1-(1-f)^2\right]V^2 \quad (13)$$

The axial loads generated by the rotors can also be computed using the axial flow momentum equation, which gives

$$T_{1-Inner} = \rho A_{1-Inner}(1-a)\left[1-(1-b)\right]V^2 \quad (14)$$

$$T_2 = \rho A_2(1-b-c)\left[(1-b)-(1-b-d)\right]V^2 = \rho A_2\, d\,(1-b-c)\,V^2 \quad (15)$$

$$T_{1-Outer} = \rho A_{1-Outer}(1-e)\left[1-(1-f)\right]V^2 \quad (16)$$

Equating equations 11–13 to equations 14–16, respectively, to obtain

$$b = 2a \quad (17)$$

$$d = 2c \quad (18)$$

$$f = 2e \quad (19)$$

The mechanical power generated by the turbine is determine from the rate of change of kinetic energy with respect to time. Therefore, the power generated by each region of the turbine is given by

$$P_{1-Inner} = 0.5\rho A_{1-Inner}(1-a)V\left[V^2 - (1-b)^2 V^2\right] = 0.5\rho A_{1-Inner} V^3\left[4a(1-a)^2\right] \quad (20)$$

$$P_2 = 0.5\rho A_2(1-b-c)V\left[(1-b)^2 V^2 - (1-b-d)^2 V^2\right] = 0.5\rho A_2 V^3(1-b-c)\left[2d-2bd-d^2\right] \quad (21)$$

$$P_{1-Outer} = 0.5\rho A_{1-Outer}(1-e)V\left[V^2 - (1-f)^2 V^2\right] = 0.5\rho A_{1-Outer} V^3\left[4e(1-e)^2\right] \quad (22)$$

Hence, the total mechanical power generation is given by

$$P = P_{1-Inner} + P_{1-Outer} + P_2$$

It can be rewritten in the power coefficient form as

$$C_P = \left(\frac{A_{1-Inner}}{A}\right)\left[4a(1-a)^2\right] + \left(\frac{A_{1-Outer}}{A}\right)\left[4e(1-e)^2\right] + \left(\frac{A_2}{A}\right)(1-b-c)\left(2d-2bd-d^2\right)$$

Let the two rotors have the same swept area, $A = A_2 = \left(A_{1-Inner} + A_{1-Outer}\right)$ and let $m = \frac{A_{1-Inner}}{A}$, we obtain

$$C_P = m\left[4a(1-a)^2\right] + (1-m)\left[4e(1-e)^2\right] + (1-b-c)\left(2d-2bd-d^2\right) \quad (23)$$

Equation 23 describes the power coefficient of a twin-rotor turbine. Let us now consider only the outer region of rotor 1, the flow in stream tube 2 is independent from any contribution of rotor 2 and can be analysed separately. Hence, for this region alone, the power coefficient can be maximized by varying the value of *e*, and the power coefficient is at the maximum when $e = \frac{1}{3}$. Therefore, the power coefficient can be rewritten as

$$C_P = m\left[4a(1-a)^2\right] + \left(\frac{16}{27}\right)(1-m) + (1-b-c)\left(2d-2bd-d^2\right) \quad (24)$$

Considering the flow in stream tube 1, the mass conservation equation gives a flow speed relationship as

$$m(1-a) = (1-2a-c) \quad (25)$$

Finally, the power coefficient can be written as a function of induction velocities *a* and *c*. This is done by substituting equation 25 into equation 24 to obtain

$$C_P = 4(1-2a-c)\left(a+c-2ac-a^2-c^2\right) + \left(\frac{16}{27}\right)\left(\frac{a+c}{1-a}\right) \quad (26)$$

3. RESULTS AND DISCUSSION

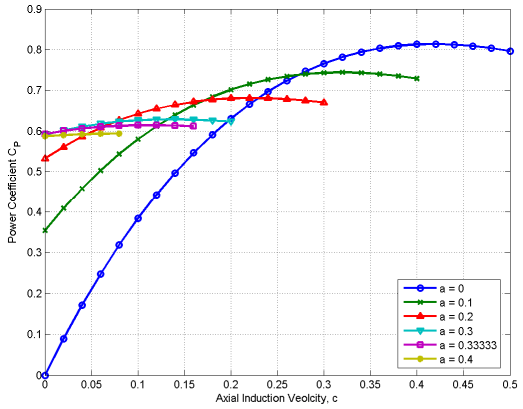

Fig.4 Power coefficient as a function of induction velocities *a* and *c*

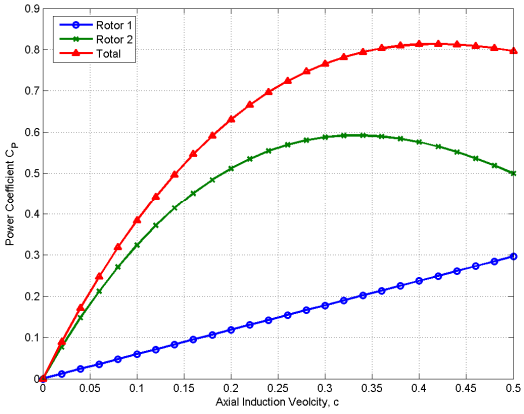

Fig.5 Power coefficient of the turbine and of each rotor at $a = 0$

Figures 4 and 5 show the variation of power coefficient with respect to changes in induction velocities *a* and *c*. The graphs have been constructed using numerical substitutions into equation 26.

Figure 4 shows the total power coefficient of the turbine when the induction velocity at rotor 2 is allowed to vary between $0 \le c \le 0.5$ and the induction velocity at the inner region of rotor 1 takes the value of $a = 0, 0.10, 0.20, 0.30, 1/3$ and 0.40. Results which do not satisfy the mass conservation conditions are not presented here.

It is found that the power coefficient is at the maximum when $a = 0$, representing zero velocity drop across rotor 1, which relates to an absence of rotor blades. Substituting the

value $a = 0$ into equation 26 gives

$$C_P = 4c(1-c)^2 + \left(\frac{16}{27}\right)c$$

The maximum power coefficient $C_{P\max}$ is calculated by differentiating the above expression with respect to rotor 2 induction velocity c. We obtain a quadratic equation $c^2 - 1.3333c + 0.382716 = 0$, whose solution is $c = 0.418$. The negative solution is physically not possible and thus ignored. The corresponding maximum power coefficient is $C_{P\max} = 0.814$ which agrees with the result shown in figure 4. Finally, the ratio of areas of rotor 1 inner and outer regions is $m = \frac{A_{1-Inner}}{A} = 0.58$.

Figure 5 shows the total power coefficient of the entire turbine and contributions from each rotor disc. It is found that when $c = \frac{1}{3}$, the power coefficient of rotor 2 C_{P2} is at the maximum and the corresponding turbine total power coefficient is $C_P = 0.79$ However, the maximum total power coefficient is actually found at $c = 0.418$ where $C_{P\max} = 0.814$. This is caused by the increase in C_{P1} due to a reduction of area within stream tube 1, i.e. an increase in area of the outer region of rotor 1.

4. DISCUSSIONS

The maximum power coefficient of the turbine found in this work is significantly higher than the value found by Newman [2]. This can be explained by the uniform flow rate past both regions of rotor 1 and rotor 2 is positioned in the wake of the inner region of rotor 1.

5. CONCLUSIONS

This study has proposed a new design in coaxial twin rotor horizontal axis turbine with a maximum power coefficient of $C_{P\max} = 0.814$ which is significantly larger than that of previous model [2]. The design proposes a 'bladeless' centre part of the upstream rotor which covers 58% of the rotor area or 76.2% of the rotor diameter. This part of the rotor only functions as a load transmitter and is not designed to extract the wind energy. See figure 6. The portion of the blade near the rotor tip is designed using the Betz theory, i.e. the velocity of the axial flow past the rotor is two-thirds of the free stream velocity. The velocity of the axial flow past the downstream rotor is 58.2% of the free stream velocity.

6. ACKNOWLEDGMENTS

The authors would like to thank Dr. Choon Tan of Gas Turbine Lab, Massachusettes Institute of Technology, whose invaluable suggestions inspired us to complete this research.

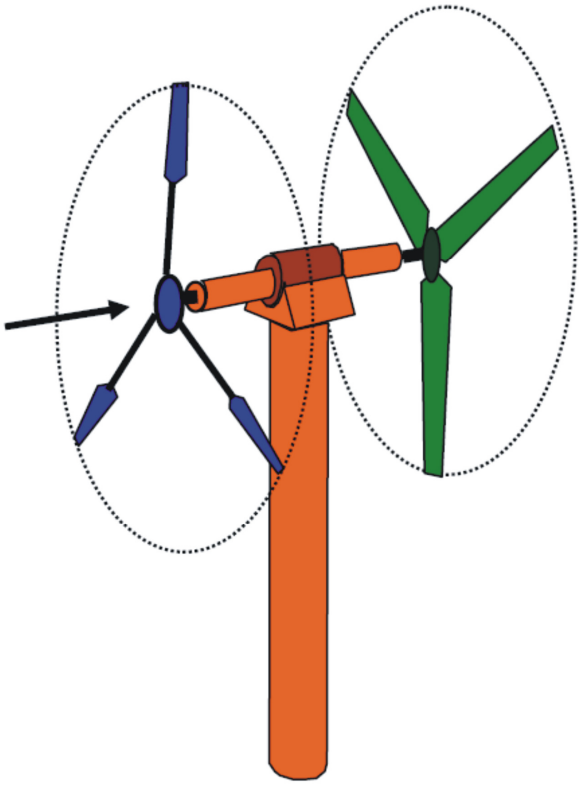

Fig.6 Illustration of the proposed design of a co-axial twin rotor horizontal axis turbine

7. REFERENCES

[1] Betz, A. (1919), *Schraubenpropeller mit Geringstem Energieverlust, Nach.der Kgl. Gesellschaft der Wiss. Zu Gottingen*, Math.-Phys. Klasse, pp. 193-217.
[2] Newman, B. G. (1983) Actuator-Disc Theory for Vertical-axis Wind Turbine, *Journal of Wind Engineering and Industrial Aerodynamics*, **15**, pp. 347-355.
[3] Newman, B. G. (1986) Multiple Actuator-Disc Theory for Wind Turbine, *Journal of Wind Engineering and Industrial Aerodynamics*, **24**, pp. 215-225.
[4] Ushiyama, I., Shimota, T. and Miura, Y. (1996), An Experimental Study of the Two-staged Wind Turbines, *Renewable Energy*, **9**, (1-4), pp. 909-912.
[5] Jung, S. N., No, T. S., and Ryu, K. W. (2004) Aerodynamics Performance Prediction of a 30 kW Counter-rotating Wind Turbine System, *Renewable Energy*, **30**, pp. 631-644.
[6] Kanemoto T. and Galal, A. M. (2006) Development of Intelligent Wind Turbine Generator with Tandem Wind Rotors and Double Rotational Armatures, *JSME International Journal*, Series B, **49**, (2)
[7] Shen, W. Z. , Zakkam, V. A. K. , Sorensen, J. N. and Appa, K. (2007) Analysis of Counter-Rotating Wind Turbines, The Science of Making Torque from Wind, *Journal of Physics: Conference Series 75* (2007)012003, 9 pages.
[8] Clarke, J.A., Connor, G., Grant, A.D. and Johnstone, C.M., 2006, Design and Testing of a Contra-rotating Tidal Current Turbine, *Proc. IMechE*, **221**, Part A: *Journal of Power and Energy*, pp. 171-179.